Isolated prompt photon production at DESY HERA

L.E. Gordon* and W. Vogelsang†
Institut für Physik, Universität Dortmund, D-44221 Dortmund, Germany
(Received 20 September 1994)

We study in detail the effects of isolation requirements on expectations for prompt photon production rates at DESY HERA in the first fully consistent study performed completely in next-to-leading order (NLO) of QCD. In particular we examine whether the isolated cross section will give useful information on the gluon content of the photon and proton. We find that the cross section turns out to be hardly sensitive to the gluon distribution of the photon in the kinematically accessible range, but that it depends significantly on the quark content of the photon in some regions of the kinematical variables. We show furthermore that the present knowledge of the proton's parton distributions, in particular, its gluon distribution, has to be improved in order to determine the photonic structure functions in this process.

PACS number(s): 13.60.Hb, 12.38.Bx, 13.85.Qk, 14.70.Bh

I. INTRODUCTION

As anticipated, first experimental data have confirmed [1] that high energy ep scattering at the DESY ep collider HERA is dominated by photoproduction processes where the electron is scattered at small angles with the emission of an almost (on-shell) real photon which scatters with the proton. These processes are particularly interesting since they are sensitive to the structure of the photon as well as of the proton. An important representative of photoproduction processes is the production of a photon at large transverse momentum p_T directly in the hard scattering.

Large-p_T prompt photon production has already been proven to be invaluable in helping to constrain the gluon distribution of the proton through experimental measurements at both fixed target facilities and hadron colliders. This is due in particular to the presence and dominance of the $qg \to \gamma q$ scattering process already in the leading order (LO), but also due to the "clean" photon signal at fixed target facilities leading to relatively precise measurements. At colliders this last advantage is somewhat diminished due to the much larger background stemming from the copious production of hadronic jets which, at given transverse momentum but for rising c.m. system (c.m.s.) energy, increases more strongly than prompt photon production as a consequence of the structure of the underlying subprocess cross sections. These jets often contain one or more π^0 which decay into photon pairs that may not be resolved by the calorimeter. Furthermore, for the same reason as above, the fraction of photons resulting from (not yet satisfactorily understood) parton-to-photon fragmentation processes is also much larger at collider energies than in fixed target experiments. In order to reduce these backgrounds and to clearly identify the photon signal suitable isolation cuts have to be performed [2, 3].

The utility of prompt photon production for providing constraints on the proton's gluon content has led to the suggestion that it may also prove useful in constraining the photonic gluon distribution at HERA [4]. In this context the process has been studied quite extensively [5–8] with the focus on different aspects of the process and on the various contributions to the cross section. The most recent and most complete such study [8] has included all contributions to the cross section in next-to-leading order (NLO), except that in that study the LO asymptotic fragmentation functions of Ref. [9] were used. The main shortcoming of [8] and all previous studies is that only the fully inclusive cross section is considered. Since, however, HERA is a collider it will be necessary to perform isolation cuts in the experiment in order to unambiguously identify the photon signal from the hadronic background, just as it is necessary at existing hadron colliders [2, 3]. This has the effect of significantly reducing the cross section due to a strong suppression of the fragmentation contributions. In order to make reliable and meaningful predictions it is most important that the theoretical calculation correctly takes into account the experimental isolation constraints.

It is expected that the first prompt photon events will soon be observed at HERA, and we thus believe that it is now time to provide a realistic theoretical study which can be directly compared to experiment. Following the success of cone algorithms to reconstruct jets at HERA [10] we anticipate that an isolation method involving a cone will also be applicable to the case of prompt photon production. In a recent paper [11] we developed an efficient analytical method to isolate photons which, for the first time, correctly treats also the fragmentation contribution in NLO. Application of this method to the recent Collider Detector at Fermilab (CDF) preliminary data [2] has given very good agreement [12] in the previously problematic low-p_T region. In this study we apply our method to the HERA situation.

*Present address: High Energy Physics Division, Argonne National Laboratory, Argonne IL 60439.
†Present address: Rutherford Appleton Laboratory, Chilton DIDCOT, Oxon OX11 0QX, England.

The layout of the rest of this paper is as follows. In Sec. II we outline the theoretical background to the calculation of the fully inclusive (i.e., nonisolated) as well as of the isolated cross section, and we give some details of our isolation method and its application to HERA. In Sec. III we present our results and in Sec. IV we give the conclusions.

II. THEORETICAL BACKGROUND

A. The inclusive cross section

As with all photoproduction processes at HERA, there are two types of contributions to the cross section, the so-called direct and resolved contributions [13]. In the direct case the photon participates directly in the hard scattering process whereas in the resolved case it interacts via its partonic structure. In the case of prompt photon production there are two further subclasses in each category, which we label the fragmentation and nonfragmentation processes (Fig. 1) according to whether the prompt photon is produced directly in the hard scattering process or via fragmentation of a final-state parton. It has been stressed elsewhere [14] that the above separation of the subprocesses according to the initial- or final-state coupling of the photon to the hard scattering partons is ambiguous and no longer well defined beyond LO. The only well-defined quantity is the sum of all the contributions where also scale dependences partly cancel out. Nevertheless we will sometimes keep the various (i.e., direct, resolved and/or fragmentation, nonfragmentation) contributions separate for convenience and for a better comparison.

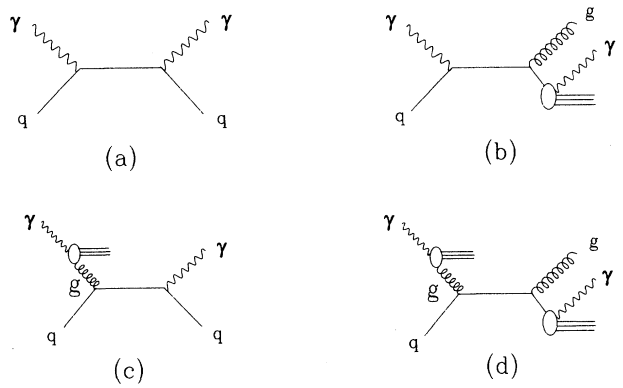

FIG. 1. Examples of (a) direct nonfragmentation, (b) direct fragmentation, (c) resolved nonfragmentation, and (d) resolved fragmentation processes (in LO) for prompt photon production at HERA.

The cross section we wish to study is $p(P_p)e^-(P_e) \to \gamma(P_\gamma)+X$. The fully inclusive cross sections can be written in the forms

$$E_\gamma \frac{d\sigma}{d^3p_\gamma} = \frac{1}{\pi S}\sum_{i,j}\int_{VW}^{V}\frac{dv}{1-v}\int_{VW/v}^{1}\frac{dw}{w}f_p^i(x_p,M^2)f_e^j(x_e,M^2) \times\left[\frac{1}{v}\frac{d\hat{\sigma}_{ij\to\gamma}}{dv}\delta(1-w)+\frac{\alpha_s(\mu^2)}{2\pi}K_{ij\to\gamma}(\hat{s},v,w,\mu^2,M^2,M_F^2)\right], \quad (1)$$

for the nonfragmentation part and

$$E_\gamma \frac{d\sigma}{d^3p_\gamma} = \frac{1}{\pi S}\sum_{i,j,l}\int_{1-V+VW}^{1}\frac{dz}{z^2}\int_{VW/z}^{1-(1-V)/z}\frac{dv}{1-v}\int_{VW/vz}^{1}\frac{dw}{w}f_p^i(x_p,M^2)f_e^j(x_e,M^2) \times\left[\frac{1}{v}\frac{d\hat{\sigma}_{ij\to l}}{dv}\delta(1-w)+\frac{\alpha_s(\mu^2)}{2\pi}K_{ij\to l}(\hat{s},v,w,\mu^2,M^2,M_F^2)\right]D_l^\gamma(z,M_F^2), \quad (2)$$

for the fragmentation part, where $S=(P_e+P_p)^2$ and $\hat{s}=x_ex_pS$ with $x_p=VW/zvw$, $x_e=(1-V)/z(1-v)$. In the latter definitions for x_p and x_e, $z=1$ is understood for the nonfragmentation case, and we have furthermore defined $V=1+T/S$, $W=-U/(S+T)$, $v=1+\hat{t}/\hat{s}$, and $w=-\hat{u}/(\hat{s}+\hat{t})$, where $T=(P_p-P_\gamma)^2$, $U=(P_e-P_\gamma)^2$, and as usual the Mandelstam variables are defined with upper case for the electron-proton system and lower case for the parton-parton system. In terms of the prompt photon's transverse momentum p_T and its HERA ep laboratory frame rapidity y, V and W are expressed by

$$1-V=\frac{p_Te^{-y}}{2E_e},\quad VW=\frac{p_Te^{y}}{2E_p}, \quad (3)$$

where E_e and E_p are the electron's and the proton's beam energies, for which we will use $E_e=30$ GeV and $E_p=820$ GeV. This fixes the photon's energy to

$$E_\gamma = p_T\cosh y = (1-V)E_e+VWE_p\ . \quad (4)$$

In Eqs. (1) and (2), $f_p^i(x_p,M^2)$ and $f_e^j(x_e,M^2)$ represent the probability of finding parton types i,j (including a photon in the electron case) in the proton and electron with momentum fractions x_p and x_e, respectively, at scale M, i.e., the proton and electron structure functions, while $D_l^\gamma(z,M_F^2)$ is the usual fragmentation function at scale M_F for the fragmentation of parton l into a photon. The first terms in the square brackets in Eqs. (1) and (2) are the LO contributions to the hard subprocess scattering cross sections, while the second terms are the NLO contributions which explicitly depend on the renormalization scale μ, the factorization scale M and the fragmentation scale M_F due to the necessity to subtract ultraviolet and collinear poles appearing in the perturbative calculation. Of course, when taking into ac-

count the NLO corrections to the cross sections in Eqs. (1) and (2), parton distributions and fragmentation functions, evolved in NLO of QCD in the same factorization scheme as that chosen in the calculation of the subprocess cross sections, have to be used in order to obtain a consistent NLO result.

We make use of the Weizsäcker-Williams approximation [15] to estimate the flux of quasireal photons from the electron beam. The structure function $f_e^j(x_e, M^2)$ is then given by the convolution

$$f_e^j(x_e, M^2) = \int_{x_e}^1 \frac{dy}{y} f_{\gamma/e}(y) f_j^\gamma \left(\frac{x_e}{y}, M^2\right) \quad , \tag{5}$$

where f_j^γ denotes the photon structure function for parton j which is thus evaluated at $x_\gamma = x_e/y$. In order to ensure that the photons participating in the reaction are almost real, and thereby justifying the use of the real-photon structure functions, we restrict the angle for the scattered electrons to be less than $\theta = 5$ degrees in the photon spectrum

$$f_{\gamma/e}(y) = \frac{\alpha_{\rm em}}{2\pi} \left[\frac{1+(1-y)^2}{y}\right] 2 \ln \frac{E_e \theta}{m_e} \quad , \tag{6}$$

where m_e is the electron mass and $\alpha_{\rm em}$ the electromagnetic coupling constant. According to the results of Ref. [16] the error introduced by using the approximation (6) at these small angles should not be greater than a few percent. Note that (6), in contrast with the full Weizsäcker-Williams spectrum used in [8], should also more closely match the experimental situation, where some sort of tagging or antitagging will almost certainly be necessary.

When the photon participates directly in the hard scattering ($j = \gamma$), the appropriate structure function must be modified. This is achieved by replacing the photon structure function $f_j^\gamma(x_e/y, M^2)$ by a δ function $\delta(1 - x_e/y)$ in Eq. (5), which leads to $f_e^\gamma(x_e, M^2) = f_{\gamma/e}(x_e)$.

In LO the subprocesses

$$q + g \to \gamma + q, \quad q + \bar{q} \to \gamma + g \tag{7}$$

contribute to the nonfragmentation part of the resolved contribution [Fig. 1(c)]. In NLO there are higher order corrections to these as well as other new processes. The subprocess cross sections for all the NLO contributions have been calculated in Refs. [17, 18] where also all the processes are listed. Both calculations were performed using the modified minimal subtraction ($\overline{\rm MS}$) factorization scheme and give identical results [18] except for minor differences which arise from the correct spin averaging for incoming gluons in the $\overline{\rm MS}$ scheme used in [18]. In our present calculation we use our own results [18] for the NLO subprocess cross sections for the resolved nonfragmentation part.

For the resolved fragmentation contributions [Fig. 1(d)], in LO the contributing subprocesses are the same as those for jet production and are listed, for example, in Refs. [6, 8]. There are many new contributions in NLO which were all calculated for inclusive hadron production in [19]. We use these subprocess cross sections in our calculation.

In the case of the direct nonfragmentation contribution [Fig. 1(a)], in LO the only process is

$$\gamma + q \to \gamma + q \quad . \tag{8}$$

In NLO we have

$$\gamma + q \to \gamma + q(+g), \quad \gamma + g \to \gamma + q + \bar{q} \quad . \tag{9}$$

Both processes have been calculated before [4], but in our calculation we obtained them from our own results [18] for the subprocess cross sections for

$$g + q \to \gamma + q(+g), \quad g + g \to \gamma + q + \bar{q} \tag{10}$$

(given in the Appendix of [18]) by removing non-Abelian couplings and adjusting color factors.

The final set of contributions we need are the direct fragmentation contributions [Fig. 1(b)] which in LO are

$$\gamma + q \to q + g, \quad \gamma + g \to q + \bar{q} \quad , \tag{11}$$

where one of the outgoing particles fragments into the photon. The NLO corrections have again both been calculated twice, first in [20] and more recently in [21]. A detailed comparison showed them to be identical [21] except again for the incoming photon and gluon spin averaging. In our calculation we use the subprocess cross sections obtained in Ref. [21] for this part of the cross section.

B. The isolated cross section

All the NLO subprocess cross sections we referred to in the preceding subsection have been calculated for the case of inclusive particle production. Thus all the momenta of the unobserved outgoing partons have been fully integrated over. This procedure does not immediately allow one to perform cuts to match the isolation criteria used in collider experiments. With the aim of correctly addressing the long-standing problem of properly including the fragmentation contributions to the isolated hadronic prompt photon cross section in NLO, we have recently developed a method of modifying the inclusive cross section by the addition of extra subtraction pieces which, when combined with the fully inclusive predictions, match the experimental definition of the isolated cross section to a high degree of accuracy [11]. Our method, which also turned out to be successful phenomenologically [12], was checked by comparison with "exact" results calculated using the more time-consuming Monte Carlo approach and was shown to be accurate over a wide range of the isolation parameters [11]. As was stressed in Ref. [11], it is the speed and simplicity of our approach which allows a consistent treatment of the NLO fragmentation contributions which are extremely long and complicated. In this subsection we briefly outline the essential aspects of our isolation method and its extension to the HERA situation and refer the reader to Ref. [11] for a detailed account.

The isolation technique used at hadron colliders is to

draw an isolation cone, radius $R = \sqrt{\Delta\phi^2 + \Delta y^2}$, around the photon, with the photon at the center, in the rapidity (y) azimuthal angle (ϕ) plane (Fig. 2). The amount of hadronic energy allowed inside the cone is then restricted to be below a certain fraction ϵ of the photon's energy, that is,

$$E_{\rm had} \leq \epsilon E_\gamma \tag{12}$$

with $E_{\rm had}$ the hadronic energy and E_γ the photon's energy. Thus we need to find some way of removing from the inclusive cross section those contributions where there is hadronic energy $E_{\rm had} \geq \epsilon E_\gamma$ in the cone around the photon. In LO where only $2 \to 2$ scattering is considered the photon is always isolated in the nonfragmentation case, while in the fragmentation case a simple cut, $z \geq 1/(1+\epsilon)$, on the fragmentation variable z appearing in Eq. (2) suffices [22]. In NLO where $2 \to 3$ scattering processes are explicitly considered, the *nonfragmentation* contributions can produce hadronic energy in the isolation cone only through a final-state parton radiating into the cone (see Fig. 2). The correctly isolated cross section must prevent such a parton from carrying more energy than ϵE_γ. We achieve the isolation of the nonfragmentation contribution by introducing a subtraction piece in the following way [11]:

$$E_\gamma \frac{d^3\sigma^{\rm isol}_{\rm nonfr}}{d^3p_\gamma}(\epsilon,\delta) = E_\gamma \frac{d^3\sigma^{\rm incl}_{\rm nonfr}}{d^3p_\gamma} - E_\gamma \frac{d^3\sigma^{\rm sub}_{\rm nonfr}}{d^3p_\gamma}(\epsilon,\delta) \quad , \tag{13}$$

where δ is the opening of a geometrical cone centered on the photon. In [11] it was shown how the subtraction cross section $E_\gamma d^3\sigma^{\rm sub}_{\rm nonfr}/d^3p_\gamma(\epsilon,\delta)$, needed for eliminating the excess hadronic energy in the cone, can be easily and accurately calculated in the small-cone approximation, i.e., by assuming that the cone around the photon is narrow. In this approximation all matrix elements can be considered in the collinear limit, assuming that the photon and the parton radiated into the cone move parallel. In those cases where a quark is collinear to the photon, the leading contribution to the subtraction piece is $O(\ln\delta)$+const for small δ, and terms of $O(\delta^2)$ and higher can be neglected. For the subprocesses $q\bar{q} \to \gamma gg$ and $qg \to \gamma qg$, however, it may be possible that a soft gluon is radiated into the cone. In this instance, although the contribution is $O(\delta^2)$, it can be potentially large due to the soft singularity in the matrix elements [22]. It turns out that this singularity is tamed by the presence of the energy resolution parameter ϵ, leading to a logarithmic dependence on ϵ [22, 11]. The final schematic form of the subtraction cross section for the nonfragmentation contributions is thus

$$E_\gamma \frac{d^3\sigma^{\rm sub}_{\rm nonfr}}{d^3p_\gamma}(\epsilon,\delta) = A\ln\delta + B + C\delta^2\ln\epsilon \quad , \tag{14}$$

where A, B, and C are functions of the kinematic variables. Simple analytic expressions for the subtraction piece are given in Ref. [11]. Let us note that in the small-cone approximation δ is related to the experimental cone size R via

$$\delta = \frac{R}{\cosh y} \quad . \tag{15}$$

In the case of the *fragmentation* contributions the situation is rather more complicated in NLO because not only the hadronic energy due to the parton fragmenting into the photon is present, but also one of the other final-state partons may come into the cone (Fig. 3). Thus in addition to the usual cut on the fragmentation variable z as in the LO case, $z \geq 1/(1+\epsilon)$, a subtraction piece is necessary to remove the excess energy from the additional parton, such that the sum of the hadronic energies in the cone satisfies Eq. (12). The fragmentation contribution to the isolated cross section may thus be written [11]

$$E_\gamma \frac{d^3\sigma^{\rm isol}_{\rm frag}}{d^3p_\gamma}(\epsilon,\delta) = E_\gamma \frac{d^3\sigma^{z\geq 1/(1+\epsilon)}_{\rm frag}}{d^3p_\gamma} - E_\gamma \frac{d^3\sigma^{\rm sub}_{\rm frag}}{d^3p_\gamma}(\epsilon,\delta). \tag{16}$$

The subprocess cross sections to be used in the fragmentation subtraction piece $E_\gamma d^3\sigma^{\rm sub}_{\rm frag}/d^3p_\gamma(\epsilon,\delta)$ were also calculated in Ref. [11] using techniques similar to those outlined above for the nonfragmentation case, and are all listed in the Appendix there. The subtraction piece has the general form

$$E_\gamma \frac{d^3\sigma^{\rm sub}_{\rm frag}}{d^3p_\gamma}(\epsilon,\delta) = \epsilon^a\left[\ln\delta(\mathcal{A} + \mathcal{A}'\ln\epsilon) + \mathcal{B}\right] \quad , \tag{17}$$

with new coefficients $\mathcal{A}$, $\mathcal{A}'$, and $\mathcal{B}$, and where $a \geq 1$. Note that in this case we have neglected the pieces $O(\delta^2\ln\epsilon)$ since these are regulated by the factor ϵ^a which causes the whole contribution to vanish as $\epsilon \to 0$.

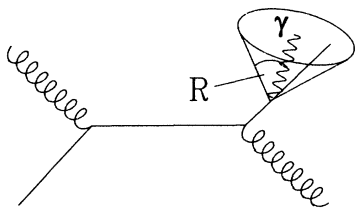

FIG. 2. Definition of the isolation cone, radius R, for prompt photon production at colliders. The figure is also an example for a nonfragmentation NLO process with hadronic energy in the isolation cone due to a parton radiating into the cone (see [11]).

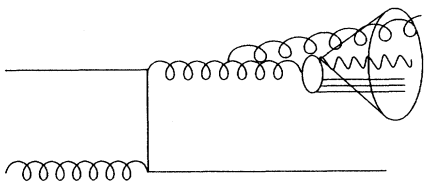

FIG. 3. Example for a NLO fragmentation process with an additional nonfragmenting parton entering the isolation cone, giving rise to additional hadronic energy in the cone (see [11]).

In Ref. [11] we have proven the good accuracy of our approximation over a wide range of the isolation parameters ϵ and δ. Although our results in [11] have been derived for the purely hadronic isolated prompt photon cross section, generalization to the HERA situation is straightforward. We only have to additionally adapt our results to the direct processes, i.e., the case of unresolved incoming photons. The subprocess cross sections for the direct nonfragmentation subtraction piece can be easily obtained from those for the resolved nonfragmentation piece listed in Ref. [11] by, as before, removing non-Abelian couplings and adjusting color factors. For the direct fragmentation subtraction piece which again takes the form (17), the subprocess cross sections are easily calculated following the method given in [11] and are also closely related to those for the resolved fragmentation subtraction piece, so we do not list them here.

This concludes our discussion of the theoretical background to the calculation. In the next section we present our results for HERA.

III. NUMERICAL RESULTS

As stated in the Introduction the main aim of this study is to see whether prompt photon production at HERA will still yield enough events in interesting and accessible kinematic regions to give useful information on the parton, and in particular the gluon, distributions in the photon and proton after isolation requirements have been taken into account. Our motivation is, of course, to address our current incomplete knowledge of these distributions particularly in the photon case, where they are a severe handicap to our ability to describe photoproduction processes, and therefore to test QCD theory in this area. Our study is the first fully consistent study of prompt photon production at HERA in NLO since for the first time fragmentation functions evolved in NLO are used. Furthermore, as mentioned before, it is the very first study altogether which deals with the experimentally relevant *isolated* prompt photon cross section at HERA.

There are now many different sets of parametrizations of the photonic parton distributions available. Most of these agree reasonably well on the quark distributions, but they can have very different gluon distributions reflecting the different assumptions made at the input scales which vary widely due to a lack of constraints on the gluon distribution. In our study we will compare predictions made with the Glück, Reya, Vogt (GRV) [23] and the Gordon, Storrow (GS) [24] photon distributions which are both available in NLO. We transform the GRV NLO parametrizations into the $\overline{\rm MS}$ scheme in order to be consistent with the choice of the factorization scheme adopted in the calculation of the various NLO subprocess cross sections. It would be expected that differences between the various proton distribution parametrizations are not likely to be significant in the regions probed by prompt photon production at HERA, since recent proton structure function measurements [25] are accommodated by all modern parametrizations. We nevertheless test this assumption by making a comparison of the predictions given by the GRV [26], Martin-Roberts-Stirling set A [MRS(A)] [27], and CTEQ2M [28] versions. For the fragmentation functions we use those of GRV, Ref. [29], which are also available in NLO. In the following we take the GRV photon and proton distributions as our standard since they match exactly in the choice of values of the QCD scale parameter Λ, and also match those of our choice of NLO fragmentation functions. Whenever different proton and photon distributions are used we always use the value of Λ corresponding to the proton distributions.

In all inclusive (i.e., nonisolated) calculations we choose the renormalization and factorization scales to be $\mu = M = M_F = p_T/2$. For isolated cross sections following the suggestion made in Ref. [22] we use Rp_T for the fragmentation scale M_F but keep the other scales as in the inclusive case. The scales $\mu = M = p_T/2$ were preferred by the CDF data on hadronic prompt photon production [12]. We work in the HERA ep laboratory frame and take positive rapidity to correspond to the proton forward direction in order to match the convention used by the HERA experimentalists [10]. We choose the energy resolution parameter $\epsilon = 0.1$ and the isolation cone size $R = 0.4$ throughout. Dependence of the (hadronic) cross section on these parameters was studied extensively in Ref. [11], and the values chosen are optimum values where our approximation is very accurate and which are still such that the reduction in the cross section relative to the inclusive case is not too severe. They are also not too far from the fixed value of $R = 0.7$ and the average value of $\epsilon = 0.15$ used by the CDF Collaboration [2] or the $R = 0.4$ of the D0 experiment [3], and should be thus applicable at HERA. We note that our values for R and ϵ are large enough to make a resummation of the logarithms in δ (or R) and ϵ appearing in Eqs. (14) and (17) unnecessary [22]. We take $N_F = 4$ active flavors throughout.

In Fig. 4(a) we show the rapidity distribution of the cross section at $p_T = 5$ GeV using our standard parton distributions. The solid curve is the fully inclusive prediction containing both resolved and direct, fragmentation and nonfragmentation contributions. The dashed curve represents the corresponding full isolated prediction. This is only shown over a rapidity range in which we are certain that our approximation is still accurate [11]. There is an approximately 15% reduction in the full cross section which is not too severe, meaning that previous conclusions [5–8] concerning the measurability of the cross section are still valid. In Fig. 4(a) we also show the effects of isolation on the fragmentation contributions only (i.e., on the sum of direct fragmentation and resolved fragmentation). The dash-dotted line is the result for the inclusive fragmentation contribution, whereas the dotted one represents the isolated fragmentation piece. In this case, as expected, the effect of isolation is a very significant reduction of this contribution relative to the inclusive case. In some respects this is a positive development since the dependence of the cross section on the poorly known fragmentation functions is correspondingly reduced leading to much "cleaner" predictions. On the other hand it also means that measurement of the cross

section at HERA will not yield any new information on the fragmentation functions if, as expected, isolation is a requirement.

Choosing a rapidity $y = 2$, a roughly central value in the asymmetrical HERA ep laboratory frame, we show in Fig. 4(b) similar curves as in Fig. 4(a) but now as a function of p_T. The effects of isolation on the cross section hardly depend on p_T. This is expected since the isolation parameters chosen do not depend on p_T. At $p_T = 5$ GeV we can expect ~ 6000 events per year if HERA reaches the integrated luminosity of $200/pb$, but due to the steep fall-off of the cross section with p_T the cross section will hardly be measurable beyond $p_T = 15$ GeV, where at most 100 events can be expected. Since we do not expect that our perturbative analysis is valid far below $p_T \sim 5$ GeV or $x_T = 2p_T/\sqrt{s} \sim 0.03$, the effective range in p_T for measurement of the cross section will be $5 \text{ GeV} \leq p_T \leq 15$ GeV.

Henceforth we shall only consider the isolated cross section. Furthermore all cross sections shown from now on will always include their respective non-fragmentation piece as well as their fragmentation contribution. In Fig. 5(a) we compare the resolved (solid line) and direct (dashed line) contributions to the isolated cross section at $p_T = 5$ GeV as a function of rapidity. Before discussing the results shown, it is interesting to observe

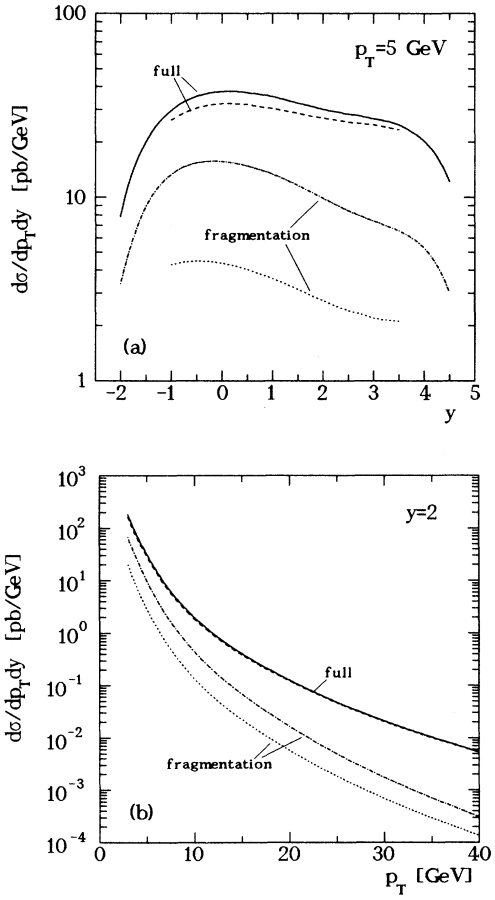

FIG. 4. (a) Comparison of the fully inclusive (solid line), full isolated (dashed line), inclusive fragmentation (dash-dotted line) and isolated fragmentation (dotted line) cross sections for prompt photon production at HERA at $p_T = 5$ GeV as a function of rapidity y. (b) Same as (a) but for p_T distributions at rapidity $y = 2$. All curves use our standard parameters as described in the text.

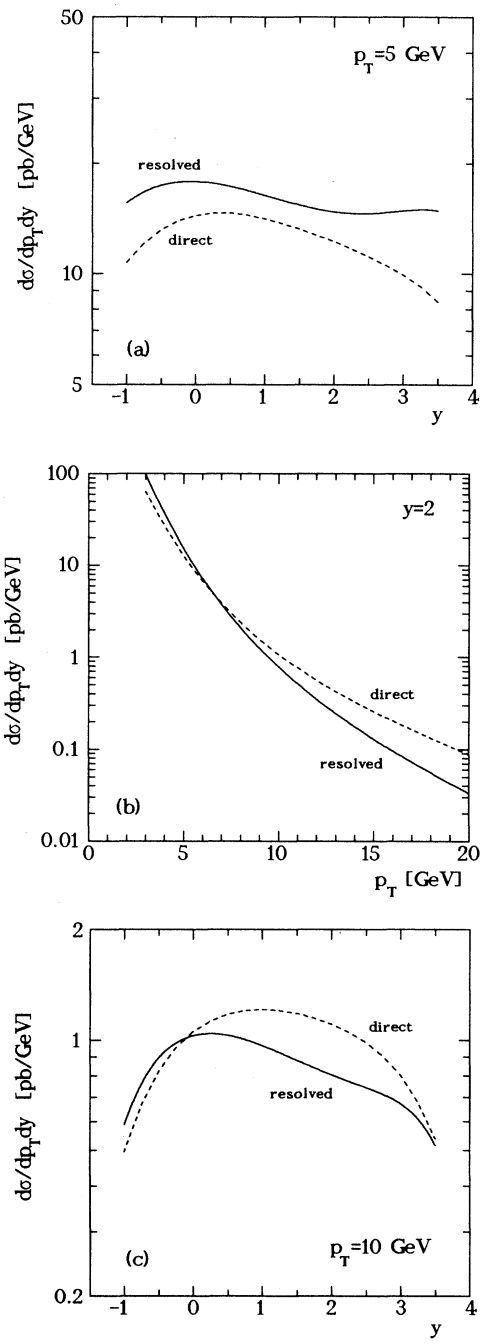

FIG. 5. (a) Rapidity distributions of the resolved (solid line) and direct (dashed line) contributions to the isolated cross section at $p_T = 5$ GeV for our standard parameters. Note that both contributions include both their respective nonfragmentation *and* fragmentation pieces. (b) Same as (a) for p_T distributions at $y = 2$. (c) same as (a) at $p_T = 10$ GeV.

from Eqs. (1)–(3) that for $p_T = 5$ GeV and $y = -1$, x_p and x_e are approximately bounded by $0.001 \leq x_p \leq 1$, $0.23 \leq x_e \leq 1$, whereas at $y = 2$ we have $0.02 \leq x_p \leq 1$, $0.01 \leq x_e \leq 1$. We see from Fig. 5(a) that the direct contribution has a peak toward the negative rapidity direction, obviously corresponding to the probing of the proton at small x_p by an energetic photon. In the case of the resolved contribution, there are two peaks. The peak at $y = 3$ should correspond to the probing of the photon distributions at small x_γ, and if, as expected, the cross section is dominated by initial quark-gluon scattering, then the cross section should be sensitive to g^γ, the photonic gluon distribution, in this region. By the same token, it should be sensitive to the quark distributions q^p at rather large x_p of the proton, in this region, so provided these are known, g^γ can be extracted in principle. The somewhat larger peak in the resolved component around $y = 0$ is, as we shall see, due to the probing of the protonic gluon distribution at small x_p by the photonic quark distributions, q^γ, at large x_γ. We shall examine these features in more detail later in this section.

Figure 5(b), which compares the resolved (solid line) and direct (dashed line) contributions as functions of p_T at $y = 2$, shows the expected dominance [8] of the direct contribution at larger p_T. We see that, even at $p_T = 5$ GeV, the resolved contribution is only slightly larger than the direct for this particular choice of structure functions. When the GS parton distributions [24] are used for the photon we find that the resolved contribution is only larger than the direct at p_T values slightly *less* than 5 GeV at $y = 2$. All this means that we can hardly expect the cross section to show much sensitivity to the photon distributions for p_T much larger than about 5 GeV. This is confirmed in Fig. 5(c) which shows the rapidity distributions at $p_T = 10$ GeV. Here we see that the direct contribution dominates at almost all rapidities. If we change the proton distributions used, to MRS(A) [27], for example, then the point at which the direct overtakes the resolved contribution is slightly increased in Fig. 5(b).

In Figs. 6(a) and (b) we check on a linear scale the sensitivity of the cross section at p_T values of 5 and 10 GeV, respectively, to the proton and photon structure functions. As stated above, we compare the results obtained for the GRV [26] (solid lines), the MRS(A) [27] (dotted lines), and the CTEQ2M [28] (dash-dotted lines) parton distributions of the proton and the GRV [23] and GS [24] photonic parton distributions. It becomes obvious that at both p_T values there is a significant normalization difference between the predictions given by the GRV and GS photonic parton distributions, but that the *shapes* of the curves (for a fixed set of proton distributions) are essentially the same. We can thus conclude that the cross section is not very sensitive to the actual shapes of the photon distributions, since the differences in the shapes of the GRV and GS distributions are known to be quite substantial at the values of Q^2 relevant here [30]. The substantial normalization differences between the two predictions can naturally be traced back to the actual sizes of both the quark and gluon distributions in each case. This difference, which can be accommodated by the available data on the photon structure function, $F_2^\gamma(x, Q^2)$, is in turn partly due to the differences in the points at which the evolution of the distributions is started, and the inputs chosen. Figures 6(a) and (b) also reveal that exploitation of this normalization difference in order to distinguish between the two parametrizations will require data with very high statistics since, as can be clearly seen, there are quite significant differences, also in the shape, between the predictions given by the various proton structure function parametrizations. We also note that there is a comparable uncertainty in the predictions due to the dependence of the cross section on the renormalization and initial state factorization scales μ, M. Using, e.g., $\mu = M = 2p_T$ instead of $p_T/2$ decreases our results in Fig. 6(a) by about 7%. In contrast with this, the dependence on the fragmentation scale M_F is very weak, as is expected for an isolated cross section [11].

Comparison of the curves obtained by using the var-

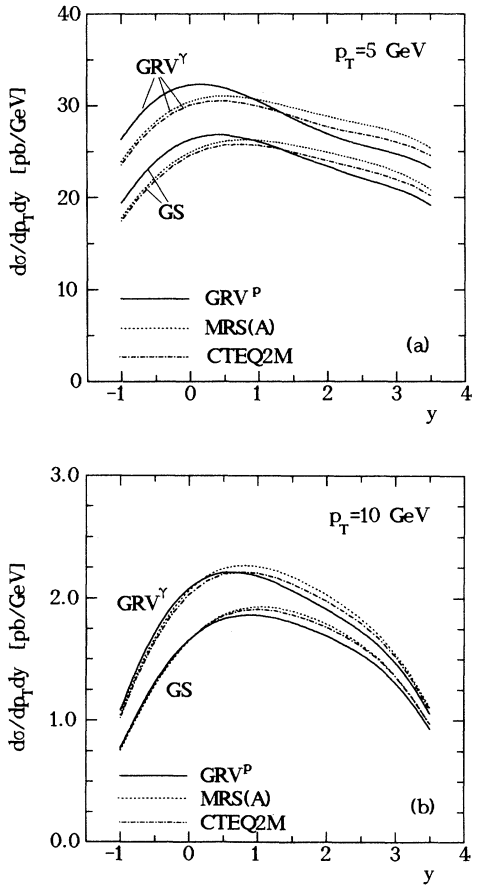

FIG. 6. (a) Rapidity distributions at $p_T = 5$ GeV of the full isolated cross section as predicted using the GRV [26] (solid lines), MRS(A) [27] (dotted lines), and CTEQ2M [28] (dash-dotted lines) parametrizations for the proton distributions. The upper curves use the GRV photon distributions [23], whereas the corresponding lower curves have been obtained with the GS photon distributions [24] as labeled. (b) Same as (a) at $p_T = 10$ GeV.

ious proton distributions reveals that the GRV proton distributions give a larger peak around $y = 0$ than either the MRS(A) or the CTEQ2M proton distributions at $p_T = 5$ GeV, but that the differences are not as significant at $p_T = 10$ GeV. This can be traced back to the steeper gluon distribution at small x_p ($x_p < 0.01$) in the GRV proton, which is probed by the $g^p q^\gamma$ scattering process. This presumption is confirmed by trying (experimentally ruled out) flat parton distributions for the proton: Choosing, for instance, the Kwiecinski-MRS set B0 (KMRS-B0) [31], one obtains a $\sim$ 40% smaller result for any of the curves in Fig. 6(a) at negative rapidities, but similar results at positive rapidities. In this respect prompt photon production at HERA could in principle serve as an independent experimental check on our present perception of a steep small-x gluon distribution of the proton, although a limit is set here by the above discussed uncertainty in the photonic parton distributions. The differences in Fig. 6(a) at positive rapidity are due partly to the gluon distributions, but more significantly to the different quark, particularly the u quark, distributions.

To further examine these issues, i.e., the dependence of the full isolated cross section on the parton content of the photon and the proton, we show in Figs. 7(a) and (b) the contributions of the various contributing scattering subprocesses at $p_T = 5$ GeV vs. rapidity. To shed more light on the proton, Fig. 7(a) presents the individual results for

$$g^p \gamma^{\text{res+dir}} \to \gamma + X$$

and

$$q^p \gamma^{\text{res+dir}} \to \gamma + X$$

scattering, where q includes quarks *and* antiquarks, and $\gamma^{\text{res+dir}}$ represents scattering of the protonic partons with resolved as well as with unresolved photons. The sum of the two above reactions of course reproduces the full isolated cross section already shown in Fig. 6(a). We show the results for the GRV (solid lines) and MRS(A) (dotted lines) proton distributions. In both cases we use the GRV photonic parton distributions. In the negative rapidity region we can clearly see that the GRV prediction is larger due to the steeper gluon distribution, confirming that the cross section is sensitive to g^p in this region. Also the MRS(A) predictions are larger at positive rapidity, which is mainly due to the slightly different size of the quark distributions. In this case the dominant quark distribution is the u-quark distribution due to its associated large charge factor, $e_u^2 = 4/9$. We see also that the differences are not as large, although still significant, for the full cross section since the two effects from the differences in q^p and g^p tend to compensate for each other.

Figure 7(b) is a similar plot analyzing in more detail the photon structure probed by the proton, for which we use the GRV parton distributions. Here we compare the results for the GRV (solid lines) and GS (dashed lines) photon distributions. The subprocesses of interest are in this case

$$p g^\gamma \to \gamma + X \ ,$$
$$p q^\gamma \to \gamma + X \ ,$$
$$p \gamma^{\text{dir}} \to \gamma + X \ ,$$

where in the last reaction γ^{dir} stands for the direct (i.e., unresolved) photon (dash-dotted line). Again the sum of the three above contributions gives the corresponding full isolated cross sections already shown in Fig. 6(a). Figure 7(b) shows that the cross section depends rather strongly on the photonic quark distributions in the direction of negative rapidities. Here the quark distributions

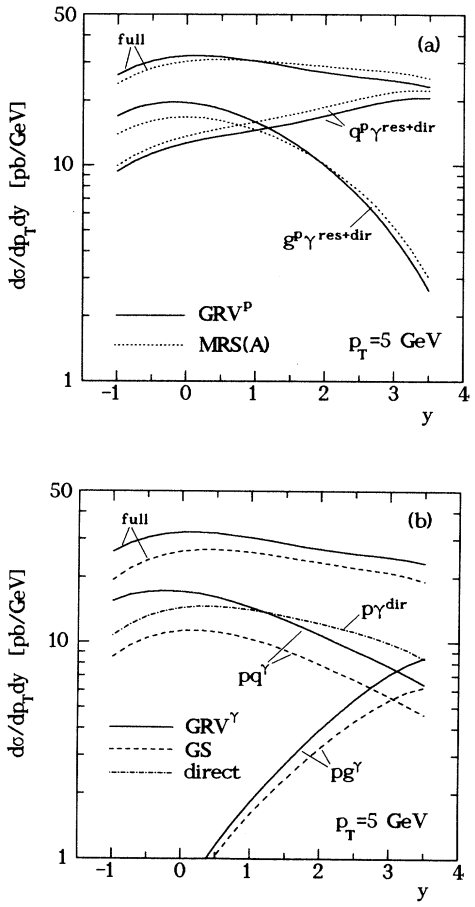

FIG. 7. (a) Comparison of the predictions given by the GRV [26] (solid lines) and MRS(A) (dotted lines) [27] proton distributions for subprocesses involving the gluon and quark structure of the *proton* when probed by the photon (see text), for which we have used the GRV [23] photon distributions. The top curves show the sums of the two subprocess contributions, which reproduce the respective full isolated cross sections already shown in Fig. 6(a). (b) Same as (a) but comparing the predictions given by the GRV [23] (solid lines) and GS [24] (dashed lines) photon distributions for subprocesses involving the gluon and the quark structure of the *photon* when probed by the proton (see text), for which we have used the GRV [26] proton distributions. The dash-dotted line shows the scattering of the proton with the direct (i.e., unresolved) photon.

q^γ are probed at large x_γ ($x_\gamma > 0.2$) and the divergence which can be seen between the results for GRV and GS is due to more steeply increasing GRV quark distributions with increasing x_γ. A similar effect for the gluon process toward positive rapidities is also due to a steeper gluon distribution, but this time with decreasing x_γ. The other main feature of the figure is that the processes involving g^γ do not dominate the cross section anywhere. In the positive rapidity region where they are most important, they are still smaller than the direct contribution and not much larger than the processes involving q^γ. We thus have to conclude that there seems to be no chance of directly measuring g^γ at HERA via prompt photon production.

IV. CONCLUSIONS

We have performed a detailed and complete study of isolated prompt photon production at the ep collider HERA fully in NLO of QCD. The results of our study indicate that, for certain choices of the isolation parameters which we believe to be reasonable, the cross section is only reduced by about 15% relative to the fully inclusive predictions, although there is a very significant reduction of the fragmentation contribution to the cross section. Furthermore, in the low-p_T region where the cross section is largest and is expected to be most sensitive to the photon structure there is a quite substantial sensitivity to the proton structure function parametrizations used, particularly to their gluon content. This tends to obscure somewhat the significant normalization differences between the predictions given by the two photon structure function parametrizations tested. We also found the cross section to be rather insensitive to the detailed shape of the photon distributions. The shape of the rapidity dependence of the cross section at negative rapidities seems to be driven to a larger extent by the protonic parton distributions, which therefore in principle might allow for experimental conclusions about the proton's gluon distribution at small x in a high-statistics experiment.

Our main conclusion is, however, that an improved knowledge of the proton's parton distributions, in the first place its gluon distribution, is necessary in order to make isolated prompt photon production at HERA a tool to determine the parton distributions of the photon. Even then, a precise determination of the gluon distribution of the photon will remain elusive. This conclusion has also been reached in Ref. [8], where the fully inclusive, i.e., nonisolated, cross section was studied. Our finding is, however, in contrast with the conclusion of Ref. [7] which also deals with the fully inclusive cross section [32], but calculated in the γp center-of-mass frame instead of the experimentally more relevant HERA laboratory frame. Our results demonstrate that this can be misleading since the introduction of the Weizsäcker-Williams spectrum [see Eq. (6)] smears out the results for γp scattering.

ACKNOWLEDGMENTS

We are thankful to E. Reya for helpful discussions. We are furthermore grateful to A. Vogt for sending us the evolution program for the NLO fragmentation functions of Ref. [29], and to J.Ph. Guillet for sending us the FORTRAN code for NLO inclusive hadron production [19]. This work was supported in part by the "Bundesministerium für Forschung und Technologie," Bonn.

[1] H1 Collaboration, T. Ahmed *et al.*, Phys. Lett. B **297**, 205 (1992); ZEUS Collaboration, M. Derrick *et al.*, *ibid.* **297**, 404 (1992); **322**, 287 (1994).
[2] CDF Collaboration, F. Abe *et al.*, Phys. Rev. Lett. **73**, 2662 (1994).
[3] D0 Collaboration, J. Kotcher, talk presented at the 9th Workshop on Proton-Antiproton Collider Physics, Tsukuba, Japan, 1993 (unpublished); J. Womersley (private communication).
[4] P. Aurenche, R. Baier, A. Douiri, M. Fontannaz, and D. Schiff, Z. Phys. C **24**, 309 (1984).
[5] A.C. Bawa and W.J. Stirling, J. Phys. G **14**, 1353 (1988).
[6] A.C. Bawa, M. Krawczyk, and W.J. Stirling, Z. Phys. C **50**, 293 (1991).
[7] P. Aurenche, P. Chiappetta, M. Fontannaz, J.Ph. Guillet, and E. Pilon, Z. Phys. C **56**, 589 (1992).
[8] L.E. Gordon and J.K. Storrow, Z. Phys. C **63**, 581 (1994).
[9] D.W. Duke and J.F. Owens, Phys. Rev. D **26**, 1600 (1982); J.F. Owens, Rev. Mod. Phys. **59**, 465 (1987).
[10] H1 Collaboration, I. Abt *et al.*, Phys. Lett. B **314**, 436 (1993).
[11] L.E. Gordon and W. Vogelsang, Phys. Rev. D **50**, 1901 (1994).
[12] M. Glück, L.E. Gordon, E. Reya, and W. Vogelsang, Phys. Rev. Lett. **73**, 388 (1994).
[13] J.F. Owens, Phys. Rev. D **21**, 54 (1980); M. Drees and F. Halzen, Phys. Rev. Lett. **61**, 275 (1988); M. Drees and R.M. Godbole, *ibid.* **61**, 682 (1988); Phys. Rev. D **39**, 169 (1989).
[14] J. Chyla, Phys. Lett. B **320**, 186 (1993); M. Greco and A. Vicini, Nucl. Phys. **B415**, 386 (1994).
[15] C.F. von Weizsäcker, Z. Phys. **88**, 612 (1934); E.J. Williams, Phys. Rev. **45**, 729 (1934).
[16] A.C. Bawa and W.J. Stirling, J. Phys. G **15**, 1339 (1989).
[17] P. Aurenche, R. Baier, A. Douiri, M. Fontannaz, and D. Schiff, Phys. Lett. **140B**, 87 (1984); P. Aurenche, R. Baier, M. Fontannaz, and D. Schiff, Nucl. Phys. **B297**, 66 (1988).
[18] L.E. Gordon and W. Vogelsang, Phys. Rev. D **48**, 3136 (1993).
[19] F. Aversa, P. Chiappetta, M. Greco, and J.Ph. Guillet, Phys. Lett. B **210**, 225 (1988); **211**, 465 (1988); Nucl. Phys. **B327**, 105 (1989).
[20] P. Aurenche *et al.*, Phys. Lett. **135B**, 164 (1984); Nucl. Phys. **B286**, 553 (1987).
[21] L.E. Gordon, Phys. Rev. D **50**, 6753 (1994).
[22] E.L. Berger and J. Qiu, Phys. Lett. B **248**, 371 (1990); Phys. Rev. D **44**, 2002 (1991).

[23] M. Glück, E. Reya, and A. Vogt, Phys. Rev. D **45**, 3986 (1992); **46**, 1973 (1993).
[24] L.E. Gordon and J.K. Storrow, Z. Phys. C **56**, 307 (1992).
[25] H1 Collaboration, I. Abt *et al.*, Nucl. Phys. **B407**, 515 (1993); ZEUS Collaboration, M. Derrick *et al.*, Phys. Lett. B **316**, 412 (1993).
[26] M. Glück, E. Reya, and A. Vogt, Z. Phys. C **53**, 127 (1992).
[27] A.D. Martin, R.G. Roberts, and W.J. Stirling, Phys. Rev. D **50**, 6734 (1994).
[28] CTEQ Collaboration, J. Botts *et al.*, Phys. Lett. B **304**, 159 (1993), now superseded by CTEQ2: J. Botts *et al.* (unpublished).
[29] M. Glück, E. Reya, and A. Vogt, Phys. Rev. D **48**, 116 (1993). Of the two NLO sets presented in this work we choose the one with an additional hadronic component at the input scale.
[30] A. Vogt, in *Workshop on Two-Photon Physics at LEP and HERA*, Proceedings, Lund, Sweden, 1994, edited by G. Jareskog and L. Jonsson (Institute of Physics, Lund University, Lund, 1994).
[31] J. Kwiecinski, A.D. Martin, R.G. Roberts, and W.J. Stirling, Phys. Rev. D **42**, 3645 (1990).
[32] It should also be noted that the study of [7] includes the LO fragmentation contribution only and thus, strictly speaking, does not represent a fully consistent NLO calculation. However, as was shown in Figs. 4(a) and (b), the fragmentation contribution is of minor importance for the full cross section even for the nonisolated (i.e., fully inclusive) case.